Transp Porous Med (2007) 70:167–179
DOI 10.1007/s11242-006-9093-0

ORIGINAL PAPER

Forced convection gaseous slip flow in circular porous micro-channels

O. M. Haddad · M. A. Al-Nimr · M. S. Sari

Received: 9 September 2006 / Accepted: 5 December 2006 / Published online: 1 February 2007

Abstract Laminar forced convection of gaseous slip flow in a circular micro-channel filled with porous media under local thermal equilibrium condition is studied numerically using the finite difference technique. Hydrodynamically fully developed flow is considered and the Darcy–Brinkman–Forchheimer model is used to model the flow inside the porous domain. The present study reports the effect of several operating parameters (Knudsen number (Kn), Darcy number (Da), Forchhiemer number (Γ), and modified Reynolds number (Re^*_D)) on the velocity slip and temperature jump at the wall. Results are given in terms of the velocity distribution, temperature distribution, skin friction ($C_f Re^*_D$), and the Nusselt number (Nu). It is found that the skin friction is increased by (1) decreasing Knudsen number, (2) increasing Darcy number, and (3) decreasing Forchheimer number. Heat transfer is found to (1) decrease as the Knudsen number, or Forchheimer number increase, (2) increase as the Peclet number or Darcy number increase.

Nomenclature

C	Coefficient in the Forchheimer term
C_f	Skin friction coefficient
C_p	Constant pressure specific heat
C_v	Constant volume specific heat
D	Diameter of the circular channel
Da	Darcy number ($K/\varepsilon\, r_0^2$)
h	Local heat transfer coefficient
K	Intrinsic permeability of the porous medium
Kn	Knudsen number (λ/r_0)

O. M. Haddad (✉) · M. A. Al-Nimr · M. S. Sari
Department of Mechanical Engineering, Jordan University of Science and Technology,
P.O. Box 3030, Irbed 22110,
Jordan
e-mail: haddad@just.edu.jo

k Thermal conductivity
k_m Overall thermal conductivity $((1-\varepsilon)k_s + \varepsilon k_f)$
p Pressure
Pe Peclet number $(Re_D{}^* Pr)$
Pr Prandtl number $(\mu C_p/k_m)$
Re_D^* Modified Reynolds number in porous media $(\rho_f u_0 D/\mu\,\varepsilon)$
R Non-dimensional transverse coordinate (r/r_0)
r Transverse (radial) coordinate
r_0 Channel radius
T Temperature of the fluid
T_m Mixing cup temperature
T_w Temperature of the wall
T_i Temperature at the inlet of the channel
t Time
t_0 Reference time $(\rho\, r_0^2/\mu)$
U Non-dimensional axial velocity (u/u_0)
u Axial velocity
u_0 Reference axial velocity $(\varepsilon\, r_0^2/\mu(-\mathrm{d}p/\mathrm{d}z))$
z Axial coordinate
Z Non-dimensional axial coordinate (z/r_0)

Greek symbols
λ Mean free path of the gas molecules
σ_v Tangential momentum accommodation coefficient
σ_T Thermal accommodation coefficient
γ Specific heat ratio (C_p/C_v)
Γ Non-dimensional Forchheimer coefficient $(\rho_f\, C\, \varepsilon^2\ (-\mathrm{d}p/\mathrm{d}z)\ r_0^4/\mu^2\, \sqrt{K})$
ε Porosity of the porous medium
μ Dynamic viscosity
ρ Density
θ Non-dimensional temperature $(T - T_i/T_w - T_i)$
θ_m Non-dimensional mixing cup temperature $(T_m - T_i/T_w - T_i)$
τ Non-dimensional time (t/t_0)
τ_w Shear stress at the wall $(-\mu\, (\partial u/\partial r)_w)$

Subscripts
f Fluid
m Mean value for the fluid
s Solid
w Wall condition

1 Introduction

Due to rapid development of modern technology, fluid flow and heat transfer in micro-channels have become interesting current research fields. Applications like accelerometers for automobile airbags, micro heat exchangers for cooling of electronic circuits, reactors for separating biological cells, pressure sensors for catheter tips, dense arrays of micro mirrors for high-definition optical displays, micro-pumps

used for inkjet printing are among many other applications in which fluid flow and heat transfer in micro-channels are involved.

Fluid flow in very small devices differs from those in macroscopic machines. The pressure gradient in long micro-ducts was observed to be non-constant and the measured flow rate was higher than that predicted from the conventional continuum flow model. This can be explained by the fact that the continuum flow model in the Navier–Stokes equations breaks down when the mean free path of the molecules is comparable to the characteristic length of the flow domain.

The Knudsen number (Kn), defined as the ratio of the molecular mean free path (λ) to the characteristic length of the system, is a measure of the degree of rarefaction of gases encountered in flows through very small channels, and also is a measure of the degree of the validity of the continuum model. The appropriate flow and heat transfer models for a given gas flow problem are dependent on the value of Knudsen number. A classification of the different gas flow regimes is given as follows: $Kn<10^{-3}$ for the continuum flow, $10^{-3}<Kn<10^{-1}$ for the slip flow, $10^{-1}<Kn<10$ for the transition flow, and $10<Kn$ for the free molecular flow (Karniadakis and Beskok 2002). As Knudsen number increases, the rarefaction effect becomes more effective and eventually the continuum assumption breaks down. Eckert and Drake (1972) have indicated that there is strong evidence to support the fact that slip flow can be modeled using the Navier–Stokes and energy equations modified by boundary conditions that contain the rarefaction effect on the velocity and temperature fields. More recently, Arkilic et al. (1994) and Liu et al. (1995) have found that the Navier–Stokes equations, when combined with velocity-slip boundary conditions, yield results for pressure drop and friction factor that are in agreement with experimental data for some micro-channel flows.

In spite of the large number of published research so far in the micro-flows literature (for more details, the reader may refer to the following review papers: Duncan and Peterson 1994; Obot 2002), many parts of the physical laws governing the fluid flow and heat transfer in micro-geometry remain unknown. Extensive experimental and theoretical studies were made in this area in order to understand the fluid behavior within these micro-devices (e.g. Araki et al. 2002; Li et al. 2002; Qu et al. 2000). Very few studies were dedicated to the flow in micro-conduits filled with porous media (Tang et al. 2005; Nield and Kuznetsov 2006). As part of a continued effort by the authors toward understanding the flow in micro-channels (Haddad et al. 2004, 2005a, b, 2006a, b, c), the objective of this study is to investigate the forced convection flow in circular micro-channels filled with porous media. The slip flow regime ($10^{-3} \leq Kn \leq 10^{-1}$) is considered and the modified extended Darcy–Brinkman–Forchheimer model is adopted to describe the thermal and hydrodynamic behavior of the flow. In this regime, the continuum model embodied in the Navier–Stokes and energy equations with first order slip/jump boundary conditions is applicable (Karniadakis and Beskok 2002).

2 Mathematical formulation

Consider a steady laminar forced convection flow of Newtonian fluid into a circular micro-channel filled with porous medium as shown schematically in Fig. 1. The flow is assumed to be hydrodynamically fully developed; that is the velocity component in the r-direction is zero and the velocity component in the z-direction (denoted by u) is

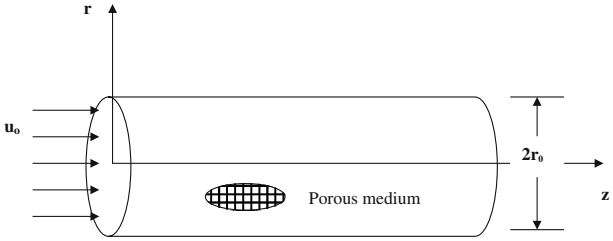

Fig. 1 Schematic diagram of the problem under consideration

function of r only. Also, it is assumed that the flow is steady and thermally developing; that is the fluid temperature is function of (r, z). In addition, the Knudsen number is considered in the slip flow regime ($10^{-3} \leq Kn \leq 10^{-1}$), therefore the Navier–Stokes equations with first order velocity slip and temperature jump boundary conditions are applicable (Karniadakis and Beskok 2002). Furthermore, this study is focused on the rarefaction effect and therefore the compressibility effect is ignored. Also, the fluid is assumed to have constant physical properties and under local thermal equilibrium condition with the solid matrix (i.e. $T_{\text{solid}} = T_{\text{fluid}} = T$). On the other hand, it is assumed that the porous medium is isotropic, rigid, and homogeneous. Under the above stated assumptions, and by using the non-dimensional variables listed in the nomenclature, the governing momentum and energy equations are reduced to the following form (Nield and Bejan 2006):
Axial momentum equation:

$$\frac{\partial U}{\partial \tau} = 1 + \frac{\partial^2 U}{\partial R^2} + \frac{1}{R}\frac{\partial U}{\partial R} - \frac{1}{Da}U - \Gamma U^2 \tag{1}$$

Energy equation:

$$U\frac{\partial \theta}{\partial Z} = \frac{1}{Pr\, Re_D^*}\left[\frac{1}{R}\frac{\partial \theta}{\partial R} + \frac{\partial^2 \theta}{\partial R^2}\right] \tag{2}$$

subject to the following boundary conditions (Gad-El-Hak 1999):

$$\text{Velocity slip:} \quad U(1) = -\frac{2-\sigma_v}{\sigma_v} Kn \left(\frac{\partial U}{\partial R}\right)_{\text{w}} \tag{3}$$

$$\text{Temperature jump:} \quad \theta(Z,1) = 1 - \frac{2-\sigma_T}{\sigma_T}\left[\frac{2\gamma}{\gamma+1}\right]\frac{Kn}{Pr}\frac{\partial \theta}{\partial R}(Z,1) \tag{4}$$

$$\text{Symmetry condition:} \quad \frac{\partial U}{\partial R}(Z,0) = \frac{\partial \theta}{\partial R}(Z,0) = 0 \tag{5}$$

$$\text{Inlet condition:} \quad \theta(Z=0, R) = 0 \tag{6}$$

where σ_v is the tangential-momentum accommodation coefficient and σ_T is the thermal accommodation coefficient, which have been determined experimentally to be between 0.2 and 0.8 (Karniadakis and Beskok 2002), where the lower limit being for exceptionally smooth surfaces while the upper limit is typical for most practical surfaces. These have been taken as $\sigma_v = \sigma_T = 0.7$ throughout the current study.

The quantities of primary interest in this study are the friction factor and Nusselt number. These are also defined as follows

$$C_{\mathrm{f}} = \frac{\tau_{\mathrm{w}}}{\frac{1}{2}\rho_{\mathrm{f}}\frac{u_0^2}{\varepsilon^2}} = \frac{\frac{\mu}{\varepsilon}\frac{\partial u}{\partial r}|_{\mathrm{w}}}{\frac{1}{2}\rho_{\mathrm{f}}\frac{u_0^2}{\varepsilon^2}} = \frac{4}{Re_D^*}\left|\frac{\mathrm{d}U}{\mathrm{d}R}\right|_{\mathrm{w}}$$

$$\therefore (C_{\mathrm{f}}Re_D^*) = 4\left|\frac{\mathrm{d}U}{\mathrm{d}R}\right|_{\mathrm{w}} \tag{7}$$

$$Nu = \frac{hD}{k_{\mathrm{m}}} = \frac{2}{1-\theta_{\mathrm{m}}}\left(\frac{\partial\theta}{\partial R}\right)_{\mathrm{w}} \tag{8}$$

where θ_{m} is the mixing cup temperature, defined as $\theta_{\mathrm{m}} = \dfrac{\int_0^1 U\theta R\,\mathrm{d}R}{\int_0^1 UR\,\mathrm{d}R}$ (9)

3 Numerical method

The governing set of differential equations are solved numerically using the finite difference technique, in which the governing differential equations are transformed into a set of algebraic equations by replacing the exact derivatives in the differential equations by their finite difference approximations. In this study, the governing momentum and energy equations are not coupled, so that the solution of the momentum equation for the velocity distribution can be obtained first, then this solution is substituted back into the energy equation to solve for the temperature distribution.

The governing momentum Eq. 1 is parabolic (unsteady, one-dimensional diffusion equation). The time term is left in the equation to solve the equation by the Time False Transient method, where the equation is assumed to be unsteady and solution proceeds until steady state solution is reached. This can be accomplished by using the well known Backward-Time-Central-Space (BTCS) method (this method is also referred to as the fully implicit method (Hoffman 1992)). To implement this, the exact derivative $(\partial U/\partial\tau)$ is replaced by its first-order-backward-time approximation, and $(\partial^2 U/\partial R^2)$ by its second-order-central-space approximation. The steady state solution is obtained by marching in time until no further significant change in the solution is obtained with additional marching steps. The present numerical method is advantageous over the other available numerical methods in that it is unconditionally stable (Hoffman 1992).

In a similar manner, the energy equation is discretized using the same numerical scheme. In contrast to the momentum equation, the steady state form of the energy equation is discretized directly and therefore a time dependent solution has not been obtained. When the momentum Eq. 1 is discretized and applied at every point in finite difference grid, a system of non-linear finite difference (algebraic) equations was obtained. To overcome the difficulties in solving such a system, the non-linear term (last term) in Eq. 1 should be linearized. To do this, the well known time lagging technique is used (Hoffman 1992).

Based on the above finite difference scheme, the resulting systems of algebraic equations (from the momentum and energy equations) are tri-diagonal. Such systems

are best solved by Thomas algorithm. For the momentum and energy equations, a uniform grid is used in both Z- and R-directions. The adequacy of the grid is verified by successive refinements of grid size until no further change in the solution is observed. For the momentum equation, it is found that a grid size of (100) points in R-direction would result in accurate solutions and any increase in number of grid points beyond this size would lead to an insignificant change in the resulting solutions. Similarly, the dimensionless time step used is based on number of refinements to ensure a time step independent solution. It is found that a time step that is equal to 0.001 or smaller would lead to invariant solutions. On the other hand, it is found that the appropriate grid size for the energy equation in (Z, R) directions is 200 $\times$ 100 points, respectively, and thus a mesh size of 200 $\times$ 100 grid points in Z- and R-directions is used throughout this study.

4 Results and discussion

To verify the current numerical results, Eq. 1 with negligible microscopic inertial term ($\Gamma = 0$) is solved analytically. The solution under such a condition is in the form

$$U(R) = \left[\frac{Da}{\left[\frac{\sigma_v - 2}{\sigma_v} \frac{Kn}{\sqrt{Da}} I_1\left(\frac{1}{\sqrt{Da}}\right) - I_0\left(\frac{1}{\sqrt{Da}}\right) \right]} I_0\left(\frac{R}{\sqrt{Da}}\right) \right] + Da$$

where I_0 and I_1 are the Bessel functions of zero and first order, respectively.

Figure 2 shows a comparison between the above analytical and the obtained numerical velocity profiles when $Da = 1.0$, $\Gamma = 0$, $Kn = 0.1$. The comparison shows that there is excellent agreement between the two solutions. In addition to this comparison, the solution for the case of no-slip flow in a clear (i.e. non-porous) circular tube is reproduced numerically by the present study and is compared with that presented

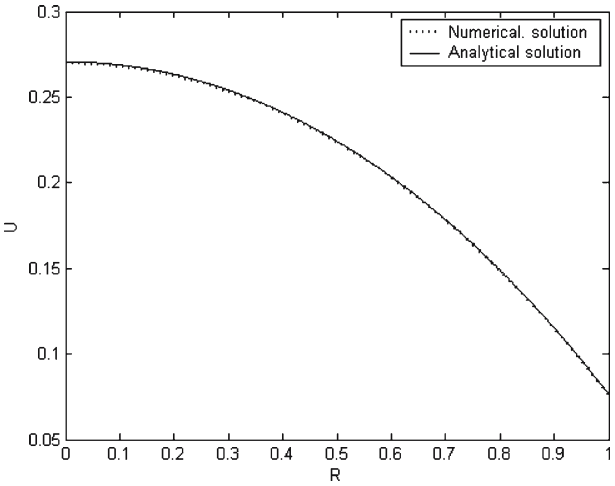

Fig. 2 Comparison between the steady state numerical and theoretical velocity profiles $Da = 1$, $\Gamma = 0$, $Kn = 0.1$

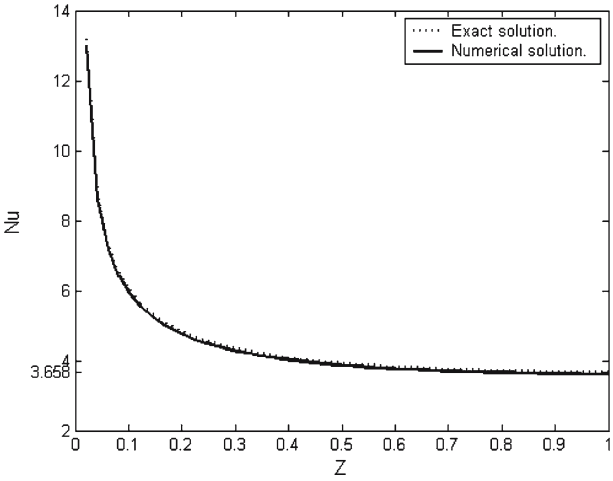

Fig. 3 Comparison between the steady state numerical and theoretical (Burmeister 1993) Nusselt number distributions: $Da = \infty, Re_D^* = 50, \Gamma = 0, Kn = 0.0$

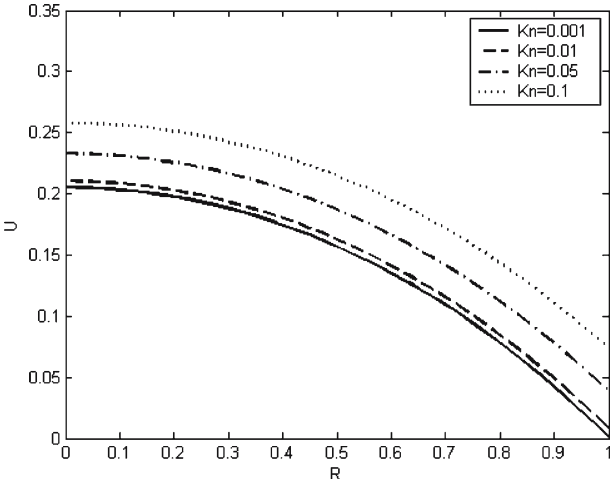

Fig. 4 Non-dimensional velocity distribution: $Da = 1, Re_D^* = 50, \Gamma = 1$

in Burmeister (1993). Figure 3 shows the comparison between the two solutions and obviously the agreement is excellent.

Figure 4 shows the effect of Knudsen number on the radial distribution of the axial velocity. It is clear that as Knudsen number increases, the velocity profile shifts up and the velocity slip at the wall is increased. This is because the increase in Knudsen number can be due to the increase in the mean free path of the molecules, and this leads to decreased retarding effect at the wall and yields larger flow rate through the channel. Also, the increase in the maximum velocity is less than that at the wall and so the velocity gradient at the wall decreases with Knudsen number. Thus, the mass flow rate increases if the pumping power is kept constant because the frictional retarding forces at the wall decrease with Knudsen number.

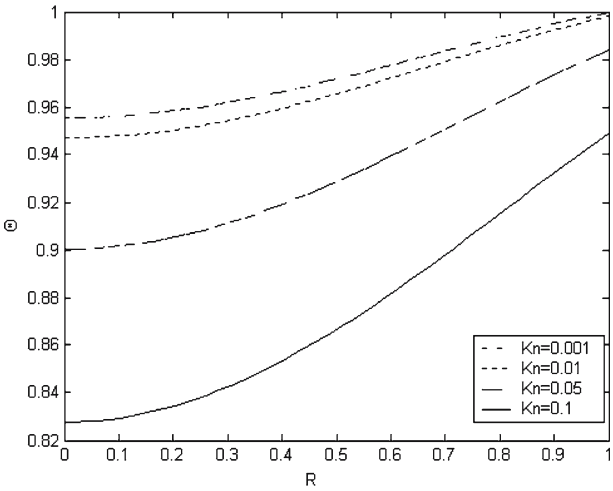

Fig. 5 Non-dimensional temperature distribution: $Z = 2$, $Da = 0.1$, $Re_D^* = 50$, $\Gamma = 0.1$

Figure 5 shows the effect of Knudsen number on the non-dimensional temperature profile. It can be noted that as Knudsen number increases, the temperature profile shifts down. This decrease in (θ) with Kn can be attributed to two effects: (a) increasing the Knudsen number means that more flow passes through the channel (i.e. the heat source at the wall must heat greater amount of fluid), (b) As Kn increases, the jump in fluid temperature at the wall increases, leading to less amount of heat transfer from the wall to the fluid. One can also observe that the effect of Kn is more significant at larger values of Kn.

Figure 6 shows the variation of $C_f Re_D^*$ with Darcy at different Knudsen numbers. The curves show that as the Knudsen number increases, $C_f Re_D^*$ decreases. It is known that any increase in Knudsen number would result in an increase in Re_D^* due to the increase in the flow velocity. On the other hand, C_f decreases due to the decrease in the velocity gradient at the wall. The net result of the effect of Knudsen number is found to decrease $C_f Re_D^*$. This means that the reduction in C_f is more significant so that it overcame the increase in Re_D^*. The effect of Knudsen number on $C_f Re_D^*$ is more significant at larger values of Knudsen number ($0.01 \leq Kn \leq 0.1$). Also, the effect of Knudsen number on $C_f Re_D^*$ is more significant at lower values of Darcy number. This implies that any change in Knudsen number at low values of Darcy number would lead to significant change in $C_f Re_D^*$. The figure also shows that as the Darcy number increases, $C_f Re_D^*$ also increases. This is because as the Darcy number increases, permeability of the porous medium increases and therefore more amount of flow enters the channel and higher velocity is obtained which lead to increase in Re_D^*. This leads the overall effect to be an increase in $C_f Re_D^*$ value.

Figure 7 shows the variation of $C_f Re_D^*$ with Forchheimer number at different values of Knudsen numbers. As noted before, the curves show that as the Knudsen number increases, $C_f Re_D^*$ decreases. The effect of the Knudsen number on $C_f Re_D^*$ is more significant at higher values of Knudsen number ($0.01 \leq Kn \leq 0.1$). Also, these curves show that as the Forchheimer number increases, $C_f Re_D^*$ remain constant and eventually decreases. Increasing the Forchheimer number decreases both Re_D^* and C_f. When the Forchheimer number increases, the microscopic inertial retarding force increases

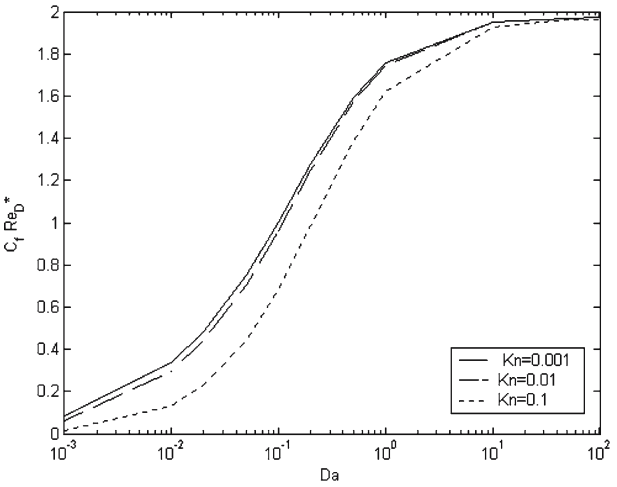

Fig. 6 Effect of Da on $C_f Re_D^*$: $\Gamma = 0.1$

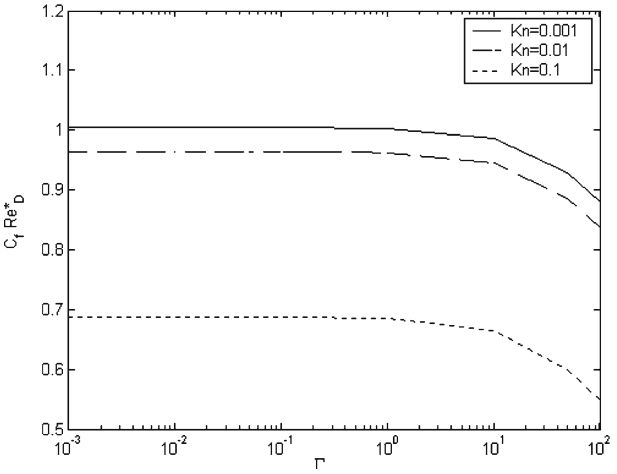

Fig. 7 Effect of Γ on $C_f Re_D^*$: $Da = 0.1$

and therefore less amount of flow enters the channel which leads to a reduction in velocity and consequently in Re_D^*. Also, as the Forchheimer number increases, C_f decreases due to the decrease in velocity gradient at the wall and as a result, $C_f Re_D^*$ will decrease.

Figure 8 shows the effect of Knudsen number on Nusselt number (Nu) distribution over the entire slip flow regime. As expected, Nusselt number decreases axially down stream because less heat transfer occurs from the wall to the fluid as the fluid is heated down stream. At large Z, the flow becomes thermally developed and Nusselt value asymptotes to a fixed value. By inspecting Fig. 8, it is clear that as the Knudsen number increases, the Nusselt number decreases due to the reduction in the heat transfer from the wall to the fluid. Increasing Knudsen number has two opposite effects on Nusselt number. The first effect is that it leads to increased velocity slip at the wall since the

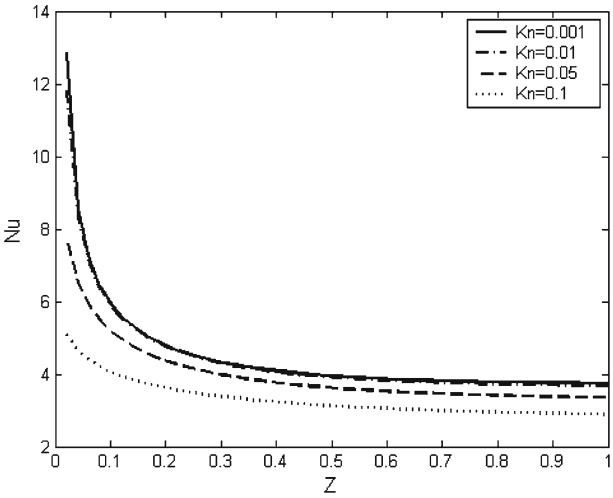

Fig. 8 Effect of *Kn* on *Nu* distribution: $\Gamma = 0.1$, $Da = 1$, $Re_D^* = 50$

velocity increases. As a result, larger flow rates are obtained or larger amounts of fluid will absorb heat from the wall, so Nusselt number increases. The second effect is that increasing Knudsen number leads to increased temperature jump at the wall. As a result, the adjacent fluid to the wall does not feel the real temperature of the wall. This results in lower heat flux from the wall to the fluid and so Nusselt number decreases. The reduction in *Nu* due to the increase in temperature jump dominates the increase in *Nu* due to the increase in fluid flow rates, and as a net result, *Nu* decreases as *Kn* increases.

Figure 9 shows the effect of Darcy number on the Nusselt number distribution at fixed values of Knudsen number. For a given Knudsen number, there are two opposite trends in the effect of Darcy number on Nusselt number in the developing and fully developed regions. As the Darcy number increases, then both velocity slip and temperature jump increases causing Nusselt number to increase and decrease respectively, regardless of the value of Knudsen number within the slip flow regime. The effect of *Da* on the velocity slip dominates the effect of *Da* on the temperature jump within the developing region. This in turn causes an increase in *Nu* number, as *Da* increases within this region, due to the increase in the gas flow rate, which causes more absorption of heat from the wall. However, the effect of *Da* on the temperature jump dominates its effect on the velocity slip within the fully developed region. This in turns causes a decrease in *Nu* number as *Da* increases due to the increase in the temperature jump, which reduces the amount of heat transfer from the wall to the fluid. Also, one may observe that the effect of Darcy number on Nusselt is insignificant at large values of *Z*. The flow needs more distance to become fully developed thermally as Knudsen number increases or Darcy number increases.

Figure 10 shows the effect of Forchheimer number on the Nusselt number distribution. For a given Knudsen number, it can be noted that there are two opposite trends in the effect of Forchheimer number on Nusselt number in the developing and fully developed regions. As the Forchheimer number increases, then both velocity slip and temperature jump decrease causing Nusselt number to decrease and increase, respec-

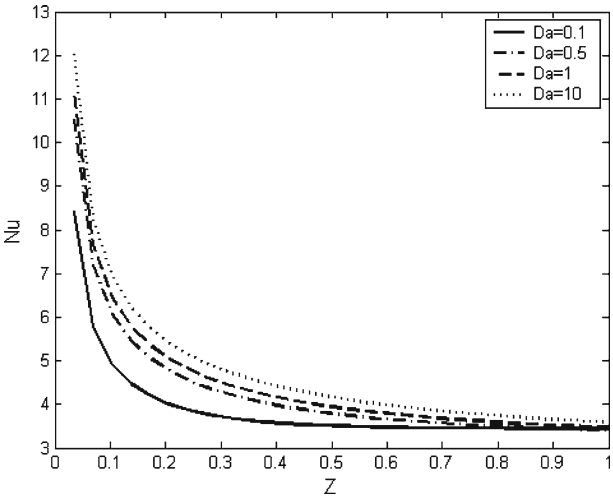

Fig. 9 Effect of Da on Nu distribution: $\Gamma = 0.1$, $Kn = 0.001$, $Re_D^* = 50$

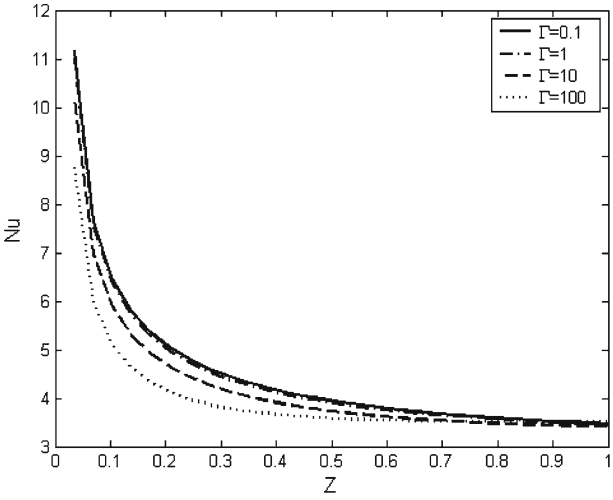

Fig. 10 Effect of Γ on Nu distribution: $Da = 1$, $Kn = 0.001$, $Re_D^* = 50$

tively, regardless of the value of Knudsen number within the slip flow regime. The effect of Γ on velocity slip is more significant in the developing region as compared with its effect on the temperature jump. As a result, increasing Γ has the effect of decreasing Nu due to the reduction in the gas flow rate. The reduction in the gas flow rate causes a reduction in the amount of heat transfer from the wall to the fluid. Now, in the fully developed region, the effect of Γ on the temperature jump is more significant as compared to its effect on the velocity slip. As a result, increasing Γ leads to an increase in Nu due to the reduction in the temperature jump at the wall. This reduction in temperature jump increases the rate of heat transfer from the wall to the fluid. Also, one may observe that the effect of Forchheimer number on Nusselt number is insignificant at large values of Z. The flow needs more distance to become

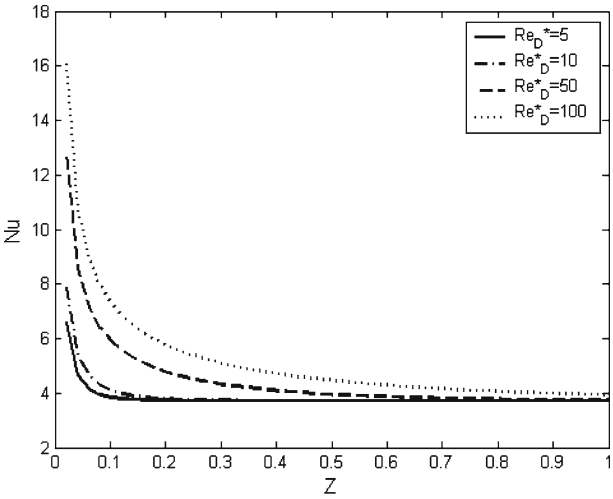

Fig. 11 Effect of Re_D^* on Nu distribution: $Da = 1, Kn = 0.001, \Gamma = 0.1$

fully developed thermally as the Knudsen number increases or Forchheimer number decreases.

Figure 11 shows the effect of modified Reynolds number on the Nusselt number distribution at specified values of Knudsen number. From this figure it can be noted that as the Reynolds number increases, the Nusselt number will increase. This is due to the increase of velocity of the fluid, and this leads to increased heat transfer by convection, and thus increased Nu number. Also, it is clear from the figure that at large values of Z, the effect of Reynolds number is insignificant.

To explain why the effect of Γ, Da, and Pe numbers on Nusselt number is insignificant at large Z, one needs to note that at large Z: $\partial\theta/\partial Z \approx 0$ as the flow become thermally fully developed. This term is multiplied by U and Pe in the energy Eq. 2, and both Γ and Da affect U directly and not θ. Therefore, if U and Pe disappear as $\partial\theta/\partial Z$ disappears then Γ, Da and Pe have no effect on θ and hence on Nusselt number Nu.

5 Conclusions

The present numerical solutions are carried out for the case of steady laminar forced convection slip flow in a circular micro-channel filled with porous medium. In this study, the slip flow regime $0.001 \leq Kn \leq 0.1$ is considered and the Darcy–Brinkman–Forchheimer model is used to model the flow inside the porous domain. The present study reports the effect of several operating parameters (e.g. Kn, Da, Γ, Pe) on the velocity slip and temperature jump at the wall. Results are given in terms of skin friction ($C_f Re_D^*$) and local Nusselt number (Nu).

It can be concluded that the skin friction is found to (1) increase as Darcy number increases (2) decrease as Forchheimer number or Knudsen number increase. On the other hand, Nusselt number is found to (1) decrease as the Knudsen number or Forchheimer number increase. (2) increase as the Peclet number or Darcy number increase.

Also, one can conclude that the thermal entrance length is shorter when Γ increases or when *Kn*, *Da* and *Pe* decrease.

References

Araki, T., Kim, M., Iwai, H., Suzuki, K.: An experimental investigation of gaseous flow characteristics in microchannels. Microscale Thermophys. Eng. **6**, 117–130 (2002)

Arkilic, E.B., Breuer, K.S., Schmidt, M.A.: Gaseous flow in microchannels, application of microfabrication to fluid mechanics. ASME FED **197**, 57–66 (1994)

Burmeister, L.C.: Convective Heat Transfer. John Wiley & Sons, New York (1993)

Duncan, G.P., Peterson, G.P.: Review of microscale heat transfer. Appl. Mech. Rev. **47**(9), 397–428 (1994)

Eckert E.G.R., Drake R.M. (1972) Analysis of Heat and Mass Transfer. McGraw-Hill, New York, 467–486

Gad-El-Hak, M.: The fluid mechanics of microdevices—the freeman scholar lecture. J. Fluids Eng. **121**, 5–33 (1999)

Haddad, O.M., Al-Nimr, M.A., Abu-Zaid, M.: Entropy generation due to laminar forced convection fluid flow through microchannel. Entropy J **6**(5), 413–426 (2004)

Haddad, O.M., Al-Nimr, M.A., AbuZaid, M.M.: The effect of frequency of fluctuating driving force on basic gaseous micro-flows. Acta Mech **179**, 249–259 (2005a)

Haddad, O.M., AbuZaid, M.M., Al-Nimr, M.A.: Developing free convection gas flow in a vertical open-ended micro-channel filled with porous media. Numer. Heat Transfer-Part A **48**, 693–710 (2005b)

Haddad, O.M., Al-Nimr, M.A., Taamneh, Y.: Hydrodynamic and thermal behavior of gas flow in microchannels filled with porous media. J. Porous Media **9**(5), 403–414 (2006a)

Haddad, O.M., Al-Nimr, M.A., AbuZaid, M.M.: Effect of periodically oscillating driving force on basic microflows in porous media. J. Porous Media **9**(7), 695–707 (2006b)

Haddad, O.M., Al-Nimr, M.A., Al-Omary, J.Sh.: Forced convection of gaseous slip flow in porous micro-channels under local thermal non-equilibrium conditions. Transp. Porous Media, published online doi:10.1007/s11242-006-9036-9 (2006c)

Hoffman, J.D.: Numerical Methods for Engineers and Scientists. McGraw Hill, New York (1992)

Karniadakis, G., Beskok, A.: Micro Flows Fundamentals and Simulation. Springer-Verlag, New York (2002)

Li, W., Lin, J., Lee, S., Chen, M.: Effect of roughness on rarefied gas flow in long microtubes. J. Micromech. Microeng. **12**, 149–156 (2002)

Liu, J., Tai, Y., Ho, C.: MEMS for pressure distribution studies of gaseous flows in micro-channels. Proc. IEEE Micro-Electro-Mechanical Syst. 209–215 (1995)

Nield, D., Bejan, A.: Convection in Porous Media. 3rd ed. Springer, New York (2006)

Nield, D., Kuznetsov, A.: Forced convection with slip-flow in a channel or duct occupied by a hyperporous medium saturated by a rarefied gas. Transp. Porous Media **64**, 161–170 (2006)

Obot, N.T.: Toward a better understanding of friction and heat transfer in microchannels – Literature review. Microscale Thermophys. Eng. **6**, 155–173 (2002)

Qu, W., Mala, Gh., Li, D.: Heat transfer for water flow in trapezoidal silicon microchannels. Int. J. Heat Mass Transfer **43**, 3925–3936 (2000)

Tang, G.H., Tao, W.Q., He, Y.L.: Gas slippage effect on microscale porous flow using the lattice Boltzmann method. Phys. Rev. E **72**(5), No. 56301 (2005)